AGU PUBLICATIONS

Paleoceanography

RESEARCH ARTICLE

10.1002/2013PA002466

Key Points:

- High-resolution SST reconstruction is performed in the westernmost Mediterranean
- Two algae-based proxies show the temperature evolution for the last 20 kyr
- Derived SSTs suggest different growth seasons of alkenone and diol producers

Supporting Information:

- Figure S1

Correspondence to:
M. Rodrigo-Gámiz,
Marta.Rodrigo@nioz.nl

Citation:
Rodrigo-Gámiz, M., F. Martínez-Ruiz, S. W. Rampen, S. Schouten, and J. S. Sinninghe Damsté (2014), Sea surface temperature variations in the western Mediterranean Sea over the last 20 kyr: A dual-organic proxy ($U^{K'}_{37}$ and LDI) approach, *Paleoceanography*, *29*, 87–98, doi:10.1002/2013PA002466.

Received 30 JAN 2013
Accepted 10 DEC 2013
Accepted article online 13 DEC 2013
Published online 11 FEB 2014

Sea surface temperature variations in the western Mediterranean Sea over the last 20 kyr: A dual-organic proxy ($U^{K'}_{37}$ and LDI) approach

M. Rodrigo-Gámiz[1,2], F. Martínez-Ruiz[1], S. W. Rampen[2], S. Schouten[2], and J. S. Sinninghe Damsté[2]

[1]Instituto Andaluz de Ciencias de la Tierra (IACT), CSIC-Universidad de Granada, Granada, Spain, [2]Department of Marine Organic Biogeochemistry, NIOZ Royal Netherlands Institute for Sea Research, Den Burg, Texel, Netherlands

Abstract A high-resolution sea surface temperature (SST) reconstruction of the western Mediterranean was accomplished using two independent, algae-based molecular organic proxies, i.e., the $U^{K'}_{37}$ index based on long-chain unsaturated ketones and the novel long-chain diol index (LDI) based on the relative abundances of C_{28} and C_{30} 1,13- and 1,15-diols. Two marine records, from the western and eastern Alboran Sea basin, spanning the last 14 and 20 kyr, respectively, were studied. Results from the surface sediments suggest that the two proxies presently reflect seasons with similar SST or simply annual mean SST. Both proxy records reveal the transition from the Last Glacial Maximum to the Holocene in the eastern Alboran Sea with an SST increase of approximately 7°C for $U^{K'}_{37}$ and 9°C for LDI. Minimum SSTs (10–12°C) are reached at the end of the Last Glacial Maximum and during the last Heinrich event with a subsequent rapid SST increase in LDI-SST toward the beginning of the Bölling period (20°C), while $U^{K'}_{37}$-SST remains constantly low (~12°C). The Bölling-Alleröd period is characterized by a rapid increase and subsequent decrease in $U^{K'}_{37}$-SST, while the LDI-SST decrease continuously. Short-term fluctuations in $U^{K'}_{37}$-SST are probably related to the availability of nutrients and seasonal changes. The Younger Dryas is recorded as a short cold interval followed by progressively warmer temperatures. During the Holocene, the general lower $U^{K'}_{37}$-derived temperature values in the eastern Alboran (by approximately 1.5–2°C) suggest a southeastward cold water migration by the western Alboran gyre and divergence in the haptophyte blooming season between both basins.

1. Introduction

A number of proxies are used to reconstruct past sea surface temperature (SST) changes resulting from past changes in climatic conditions. One of the earliest proxies that was developed is the stable oxygen isotopic composition of preserved carbonate shells of planktonic foraminifera [e.g., *Shackleton*, 1967; *Erez and Luz*, 1983]. The Mg/Ca ratio in foraminifera [e.g., *Nürnberg et al.*, 1996; *Elderfield and Ganssen*, 2000] and the application of transfer functions and modern analog techniques (MAT) on fossil foraminiferal assemblages [e.g., *Kallel et al.*, 1997a; *González-Donoso et al.*, 2000; *Pérez-Folgado et al.*, 2003; *Kucera et al.*, 2005; *Essallami et al.*, 2007; *Sicre et al.*, 2013] have also been commonly used as SST proxies for paleoceanographic studies. In addition, several organic proxies have been developed for SST reconstruction [*Brassell et al.*, 1986; *Schouten et al.*, 2002; *Rampen et al.*, 2012].

Long-chain alkenones (C_{37}, C_{38}, and C_{39}) were identified in marine sediments by *de Leeuw et al.* [1980], and *Volkman et al.* [1980] identified a specific group of marine phytoplankton, i.e., haptophytes (*Emiliania huxleyi*), as their source. Subsequently, other haptophytes, genetically closely related to *E. huxleyi*, were also identified as alkenone producers [e.g., *Marlowe et al.*, 1984; *Prahl and Wakeham*, 1987; *Conte et al.*, 1998]. *Brassell et al.* [1986] realized the potential of alkenones for reconstructing paleotemperatures and defined the $U^{K'}_{37}$ index based on the relative abundances of C_{37} di-, tri-, and tetra-unsaturated ketones, which was later simplified by exclusion of the $C_{37:4}$ alkenone [*Prahl and Wakeham*, 1987; *Prahl et al.*, 1988]. The $U^{K'}_{37}$ index is converted to SST using a global core-top calibration [*Müller et al.*, 1998], although in some regions, such as the Mediterranean, local calibrations have been developed [*Ternois et al.*, 1997; *Conte et al.*, 2006]. The $U^{K'}_{37}$ has been widely applied in paleoceanographic studies for at least two decades and is commonly applied on sediments spanning the last 3.5 Ma [e.g., *Herbert et al.*, 2010].

Long-chain alkyl diols are another group of widely occurring lipids in marine sediments and are dominated by C_{28} and C_{30} 1,13-diols, C_{28} and C_{30} 1,14-diols, and C_{30} and C_{32} 1,15-diols [*Versteegh et al.*, 1997]. C_{28} and C_{30} 1,14-diols have been identified in *Proboscia* diatoms [*Sinninghe Damsté et al.*, 2003; *Rampen et al.*, 2007] and in the marine alga *Apedinella radians* [*Rampen et al*., 2011], while C_{28} and C_{30} 1,13-diols and C_{30} and C_{32} 1,15-diols have been reported in eustigmatophyte algae [*Volkman et al*., 1992, 1999; *Gelin et al*., 1997; *Méjanelle et al*., 2003]. However, since eustigmatophytes are not widely reported in open ocean settings, uncertainty exists about the biological source of long-chain 1,13- and 1,15-diols [*Versteegh et al*., 1997, 2000]. Recently, a novel long-chain diol index (LDI), based on the fractional abundances of C_{30} 1,15-diol relative to those of C_{28} 1,13-, C_{30} 1,13-, and C_{30} 1,15-diols, was proposed as a paleothermometer [*Rampen et al*., 2012]. In a large set of surface sediments, mainly from the North and South Atlantic Ocean, the LDI showed a strong linear correlation with SST over a temperature range of −3 to 27°C. In a marine core from the Congo River outflow, the LDI provided a SST reconstruction over the last 43 kyr, reflecting known climatic events, which was in good agreement with the $U^{K'}_{37}$-SST record [*Schefuß et al*., 2005; *Rampen et al*., 2012]. A recent study showed a LDI-reconstructed SST record off southern Australia for the last 135 kyr that generally was similar to the $U^{K'}_{37}$, TEX^{H}_{86}, and foraminiferal assemblage SST records [*Lopes dos Santos et al*., 2013]. Some differences were noted in absolute SST estimates probably because the different proxies reflect SST of different seasons. Thus, the combination of diverse organic paleothermometers in marine records provides complementary information for paleoclimate and paleoceanographic reconstruction studies.

Here we present a SST reconstruction for the westernmost Mediterranean for the last 20 kyr using a dual-organic proxy approach ($U^{K'}_{37}$ and LDI). Previous SST reconstructions of the Mediterranean Sea were mainly based on $U^{K'}_{37}$ in combination with $\delta^{18}O$ values of planktonic foraminifera [e.g., *Cacho et al*., 1999, 2001, 2002; *Emeis et al*., 2000; *Martrat et al*., 2004, 2007]. More recently, a combination of $U^{K'}_{37}$ and TEX_{86} proxies has been applied in the western and central Mediterranean to reconstruct temperatures for the last few millennia [*Grauel et al*., 2013; *Nieto-Moreno et al*., 2013] and the penultimate interglacial to glacial cycle (from 244 to 130 kyr) [*Huguet et al*., 2011], and in the eastern Mediterranean for the last 30 kyr [*Castañeda et al*., 2010]. In general, these SST reconstructions have revealed a temperature gradient between the colder western and the warmer central Mediterranean and Levantine basin, as well as a close connection of the short-term Mediterranean climate and oceanographic variability with North Atlantic fluctuations [*Cacho et al*., 1999, 2001; *Martrat et al*., 2004, 2007; *Essallami et al*., 2007; *Boussetta et al*., 2012]. We studied two marine cores from the Alboran Sea basin to (1) obtain a continuous record of SST at high resolution for the last 20 kyr, (2) to test the relevance of the novel LDI proxy in marine records from midlatitude areas, and (3) to obtain additional information about potential seasonal effects on SST records using algae-derived organic proxies. We also discuss the response of these organic proxies on influences from the North Atlantic inflow and the specific Mediterranean thermohaline circulation in the Alboran basin.

2. Material and Methods

2.1. Study Area and Recovered Cores

The Alboran Sea basin presents a particular hydrodynamic feature, with the Atlantic jet interacting with the more saline and denser Mediterranean water. The Atlantic surface water (ASW) flows through the Strait of Gibraltar into the Alboran Sea from the west at the surface (200 m) and mixes with the Mediterranean water, forming the modified Atlantic water (MAW), flowing out the Mediterranean at depth. The ASW, which is almost homothermal (15°C), describes two near permanent anticyclonic gyres, namely, the western Alboran gyre (WAG) and the eastern Alboran gyre (EAG) [*Millot*, 1999], being the most characteristic features of the surface circulation in the Alboran Sea (Figure 1). Below the MAW, the Levantine intermediate waters (LIW) (200–600 m) and the deeper western Mediterranean deep water (WMDW) (>600 m) come from the east. The Mediterranean outflow water is formed through the Strait of Gibraltar, where a major proportion of LIW mixes with WMDW [*Send et al*., 1999] forming an outflow water mixed between eastern and western basins (Figure 1). Thus, both cores recovered are situated in a strategic position; i.e., the 434G core is located at the northern edge of the WAG and the 293G core in the transition to the EAG. These gyres show a high annual-interannual variability driven mainly by the position of the atmospheric pressure cells and the formation of high-fertility waters with enhanced production at the northern edge of the WAG [*Sarhan et al*., 2000].

The two analyzed gravity cores were recovered in the Alboran Sea (Figure 1). Core 293G (402 cm) was recovered from the east Alboran Sea basin (latitude: 36′10.414N, longitude: 2′45.280W; depth 1840 m below sea level (mbsl)) during the Training Through Research (TTR) 12 cruise. The inorganic geochemical, mineralogical, and grain size distribution records from this record have been reported by *Rodrigo-Gámiz et al*. [2011]. A

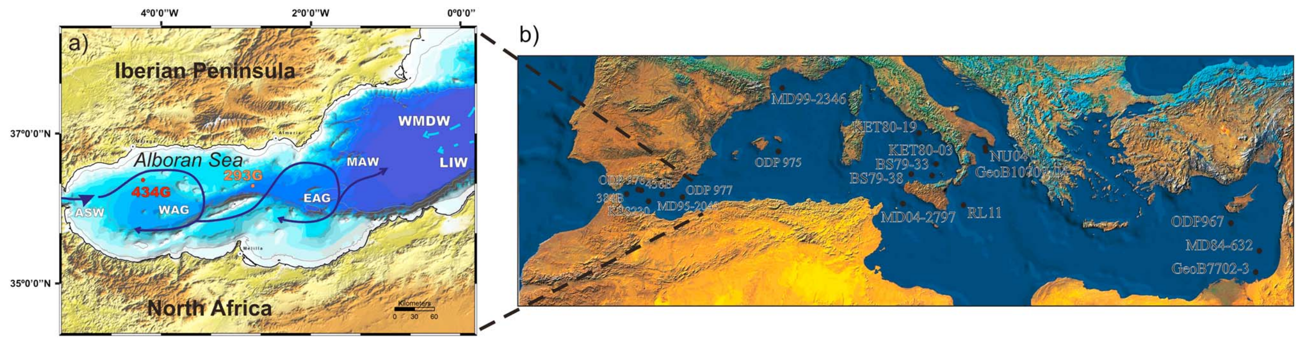

Figure 1. (a) Map of the studied area with localization of the two gravity cores studied, the 434G setting recovered in the western Alboran basin and the 293G setting in the eastern Alboran Sea basin. Dark blue arrows represent the theoretical surface circulation in the Alboran Sea: Atlantic surface water, western Alboran gyre, eastern Alboran gyre, and Modified Atlantic Water. Gray arrows represent deepwater mass circulation: the Levantine Intermediate Water and the western Mediterranean deep water. (b) Map of the Mediterranean Sea with the position of other marine records cited in the text, wherein either organic or inorganic temperature proxies were carried out from the western to the eastern Mediterranean: ODP 976 and ODP975 [*González-Donoso et al.*, 2000]; 384B and 436B [*Nieto-Moreno et al.*, 2013]; KS8230, RL11, and ODP967 [*Emeis et al.*, 2000]; ODP 977 [*Martrat et al.*, 2004, 2007; *Huguet et al.*, 2011]; MD95-2043 [*Cacho et al.*, 2001, 2002; *Martrat et al.*, 2004, 2007]; MD99-2346 [*Melki et al.*, 2009; *Boussetta et al.*, 2012]; KET80-19 and KET80-03 [*Kallel et al.*, 1997a]; BS79-38 and BS79-33 [*Cacho et al.*, 2001, 2002]; MD04-2797 and MD84-632 [*Essallami et al.*, 2007; *Sicre et al.*, 2013]; NU04 and GeoB10709-04 [*Grauel et al.*, 2013]; and GeoB7702-3 [*Castañeda et al.*, 2010].

second gravity core, 434G (252.5 cm), was recovered at Ocean Drilling Program (ODP) Site 976 [*Comas et al.*, 1996] in the west Alboran Sea basin (latitude: 36'12.313N, longitude: 4'18.735W; depth 1108 mbsl) during the TTR-17 (R/V *Professor Logachev*) cruise. The lithology of both marine sequences is dominated by homogeneous green-brownish hemipelagic mud-clays with some foraminifera and shell fragments [*Comas and Ivanov*, 2003].

2.2. Chronology and Oxygen Isotope Stratigraphy

The chronology of core 293G was originally established by *Rodrigo-Gámiz et al.* [2011] using 10 accelerator mass spectrometry (AMS) ^{14}C dates, and two additional ones (Table 1) were obtained in order to provide a higher accuracy and robustness of critical intervals in the record. The age model of the gravity core 434G is based on linear interpolation of seven AMS radiocarbon dates of picked specimen ($>$125 μm; 10 mg) of the planktonic foraminifera *Globigerina bulloides*, analyzed at the Poznan Radiocarbon Laboratory (Poland) (Table 1 and Figure 2). For both cores, the radiocarbon ages were calibrated to calendar years (cal years B.P., with 0 B.P. equivalent to A.D. 1950) using Calib 6.0.2 software [*Stuiver and Reimer*, 1993] and the Marine09 calibration curve, with a correction for ocean surface reservoir effects of 400 years [*Reimer et al.*, 2009], except for the time period spanning the last 17–15 kyr where a 815 year reservoir effect was applied according to *Siani et al.* [2001]. Similar age models were obtained using the OxCal software, but for consistency with previous studies, we used the age model obtained with the Calib software. Mean sedimentation rates obtained using these age models are 18.5 cm/kyr for core 434G (Figure 2) and 20.0 cm/kyr for core 293G [*Rodrigo-Gámiz et al.*, 2011].

Foraminiferal stable oxygen isotope compositions (δ^{18}O) in core 293G were determined on *G. bulloides* from the fraction $>$125 μm. The shells were analyzed using a Finnigan MAT 252 mass spectrometer with an

Table 1. Results of AMS ^{14}C Carbon Dating of Single Planktonic Foraminifera *Globigerina bulloides* ($>$125 μm) Picked From Cores 434G and 293G

Sample Description	Core Depth (cm)	Laboratory Code	^{14}C AMS Age (B.P.)	Calibrated Age (cal years B.P.) (Range 2σ)[a]
434G 0 27–28.5	27.75	Poz-40736	1350 ± 35	788–970
434G 1 30–31.5	66.75	Poz-40737	3350 ± 40	3090–3331
434G 2 18–19.5	108.75	Poz-40738	4680 ± 40	4819–5020
434G 3 27–28.5	173.75	Poz-40739	7960 ± 50	8329–8535
434G 4 15–16.5	217.25	Poz-44172	10,100 ± 90	10,762–11,244
434G 4 30–31.5	232.25	Poz-47037	11,140 ± 60	12,550–12,774
434G 4 49.5–51	251.75	Poz-37154	12,200 ± 70	13,440–13,808
293G 5 9–10.5	241.75	Poz-47104	10,760 ± 80	11,909–12,407
293G 6 30–31.5	320.75	Poz-47105	12,940 ± 70	14,219–15,110

[a]Ages were calibrated using Calib 6.0.2 software and Marine09 calibration curve (data from 2 σ probability interval).

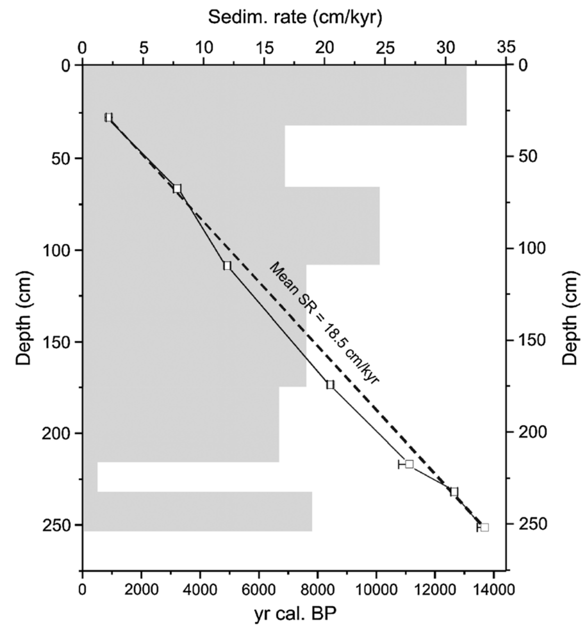

Figure 2. Sedimentation rates along 434G sediment core calculated linearly by seven AMS ^{14}C ages (open squares) calibrated with Calib 6.0.2 software [*Reimer et al.*, 2009] (see Table 1 for details). The mean sedimentation rate of 18.5 cm/kyr is represented by dashed line.

analytical reproducibility of <0.07‰ and reported in the conventional notation with reference to Vienna Pee Dee belemnite standard [see *Rodrigo-Gámiz et al.*, 2011].

2.3. Biomarker Analysis

Core 434G was sampled continuously at 3 cm intervals and at 1.5 cm intervals for the first 16.5 cm (Late Holocene) and some critical intervals such as the Younger Dryas (YD) and Alleröd period ($n = 92$), while core 293G was sampled each 6 cm for the time interval spanning the Holocene, and each 1.5 to 3 cm for the first 13.5 cm (Late Holocene) and the time intervals corresponding to the YD, Bölling-Alleröd (B-A) period, and the last Heinrich event (H1) ($n = 97$).

Freeze-dried sediment samples were homogenized in agate mortar and subsequently extracted with an Accelerated Solvent Extractor (Dionex ASE 200) using a solvent mixture of 9:1 (vol/vol) dichloromethane (DCM) to methanol (MeOH) at 100°C and 7.6×10^6 Pa. The solvent of the extract was removed by rotary evaporation. The extracts were separated into apolar, ketone, and polar fractions by column chromatography using a Pasteur pipette filled with Al_2O_3 (activated for 2 h at 150°C) using 9:1 (vol/vol) hexane/DCM, 1:1 (vol/vol) hexane/DCM, and 1:1 (vol/vol) DCM/MeOH as the eluents, respectively.

2.3.1. Alkenone Analysis

The ketone fraction was dried under N_2 and redissolved in a small volume (20–100 μL) of hexane. Quantification of the di- ($C_{37:2}$) and tri-unsaturated ($C_{37:3}$) alkenones was performed on a Hewlett Packard 6890 Gas Chromatograph (GC) using a 50 m CP Sil-5 column (0.32 mm diameter, film thickness of 0.12 μm), equipped with flame ionization detector and helium as the carrier gas, following GC conditions as described by *Castañeda et al.* [2010]. Alkenone relative abundances were determined by the integration of relevant peak areas. The $U^{K'}_{37}$ index (equation (1)) was used to estimate SST [*Prahl et al.*, 1988].

$$U^{K'}_{37} = [C_{37:2}]/([C_{37:2}] + [C_{37:3}]) \tag{1}$$

$U^{K'}_{37}$ values were converted to SSTs using the global core-top calibration proposed by *Müller et al.* [1998]:

$$U^{K'}_{37} = 0.033 \times SST + 0.044 \tag{2}$$

For core 434G, 49 of the 92 samples were run in duplicate while 39 of the 97 samples from core 293G were run in duplicate and 4 samples were run in triplicate. The mean standard deviation (SD) of the $U^{K'}_{37}$ is 0.01, equivalent to 0.3°C.

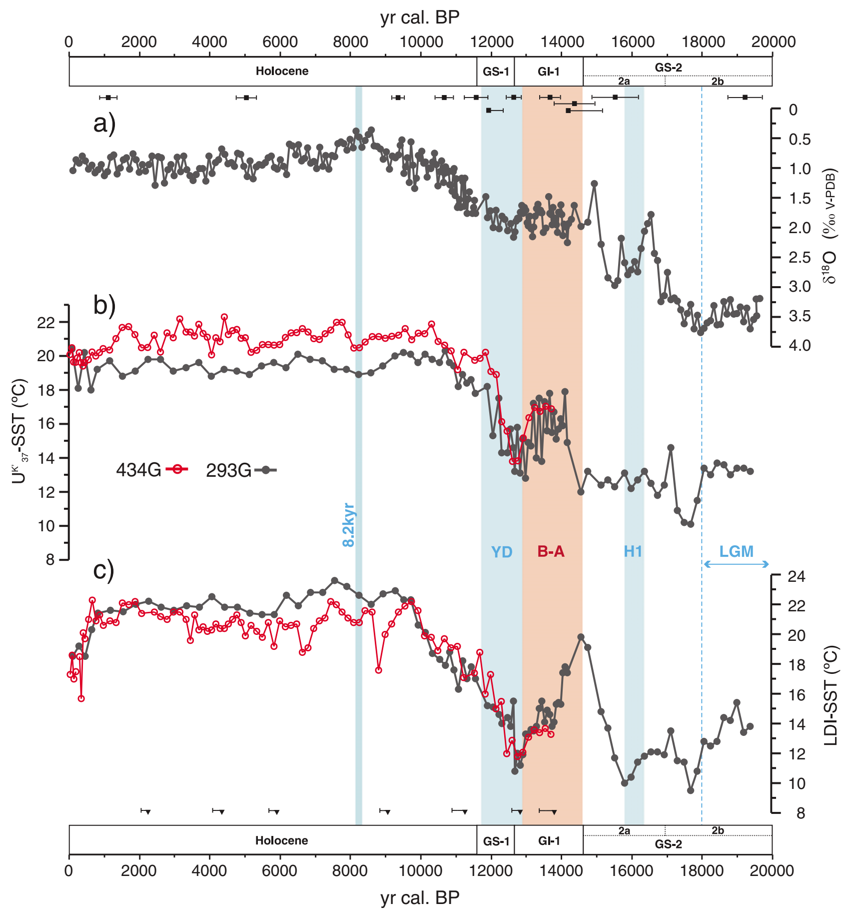

Figure 3. Records of $\delta^{18}O$ of the planktonic foraminifera *G. bulloides* [*Rodrigo-Gámiz et al.*, 2011] of (a) core 293G, (b) $U^{K'}_{37}$-, and (c) LDI-SST for cores 293G in the eastern Alboran (gray circles) and 434G (open red circles) in the western Alboran Sea. The light red vertical bar indicates the warm period Bölling-Alleröd. The short dashed blue vertical line indicates the end of the Last Glacial Maximum time interval. Light blue bars indicate main cold periods, i.e., the last Heinrich event [*Sierro et al.*, 2005], and the "8.2 kyr" cold event [*Alley et al.*, 1997]. White horizontal boxes along the *x* axis indicate Greenland stadials (GS-1 and GS-2), interstadials 1, and Holocene. Chronostratigraphy timing subdivisions are based on ^{14}C AMS dates (squares and inverted triangles plotted in Figures 3a and 3c from cores 293G and 434G, respectively) and stable oxygen isotope stratigraphy from Greenland ice cores published by *Stuiver and Grootes* [2000], *Björck et al.* [1996], and *Lowe et al.* [2008].

2.3.2. Long-Chain Diol Analysis

Aliquots of the polar fractions were dried under N_2, silylated by adding 15 μL N,O-bis(trimethylsilyl) trifluoroacetamide and pyridine and heating in an oven at 60°C for 20 min, and dissolved in 50–100 μL ethyl acetate, and long-chain diols were analyzed using GC mass spectrometry as described by *Rampen et al.* [2012]. Different long-chain diols were quantified using selected ion monitoring of *m/z* 313 and 341. The long-chain diol index was calculated and converted to SST following the relation and equation by *Rampen et al.* [2012], which is based on more than 200 surface sediments distributed globally:

$$\mathrm{LDI} = [\mathrm{C}_{30}\,1,15\text{-diol}]/([\mathrm{C}_{28}\,1,13\text{-diol}] + [\mathrm{C}_{30}\,1,13\text{-diol}] + [\mathrm{C}_{30}\,1,15\text{-diol}]) \quad (3)$$

$$\mathrm{LDI} = 0.033 \times \mathrm{SST} + 0.095 \quad (4)$$

Replicate ($n = 29$) and triplicate ($n = 3$) analysis of samples from both cores showed a mean SD for the LDI of 0.02, equivalent to 0.5°C.

3. Results

For core 293G, $U^{K'}_{37}$-SST estimates vary between 10 (end of the Last Glacial Maximum (LGM), 17.7 cal kyr B.P.) and 20°C (Late Holocene) (Figure 3b). The B-A period shows rapid $U^{K'}_{37}$-SST fluctuations between 13 and 18°C in a similar pattern as observed for the $\delta^{18}O$ values of planktonic foraminifera (Figure 3a). The $U^{K'}_{37}$-SSTs for core 434G follow those observed for 293G but are approximately 2°C higher during most of the Holocene (Figure 3b).

LDI-derived SST records show a similar trend as the $U^{K'}_{37}$-SST records (Figure 3c). For core 293G, minimum SSTs (approximately 9°C) are recorded at the end of the LGM and during H1. A marked increase is observed at the onset of the Bölling, reaching 20°C, followed by a progressive decrease during the Alleröd to reach minimum SST (11°C) at the onset of the YD. From here, SST increases at a constant rate until approximately 9.7 cal kyr B.P. Subsequently, SST values remain rather stable at approximately 22°C, except for the most recent sediment horizons that reveal lower SST estimates. The LDI-SST record of core 434G shows a similar evolution with slightly lower SST values in the mid-Holocene compared to 293G (Figure 3c).

4. Discussion

4.1. Comparison of the $U^{K'}_{37}$ and LDI Proxies

Considering the calibration errors, the two proxies applied yield similar temperature estimates (~17–20°C) for the surface sediments, which are in line with annual mean but also with spring and autumn SST in the west and east Alboran basin (18.0°C–18.5°C, 17.4°C–17.8°C, and 18.0°C–18.2°C, respectively; Table 2).

In previous studies, comparison of $U^{K'}_{37}$ temperature records with seasonal SST reconstructions based on foraminiferal fauna in the Alboran Sea have shown that the $U^{K'}_{37}$ temperature lies close to annual mean or autumn-spring temperatures during the last 8 kyr and during the B-A period, but is higher for the LGM, suggesting that seasonal variations in alkenone production have played a role in the $U^{K'}_{37}$ records (see Figure 1 supporting information) [*Sbaffi et al.*, 2001; *Pérez-Folgado et al.*, 2003; *Essallami et al.*, 2007; *Sicre et al.*, 2013]. Furthermore, fluxes of *E. huxleyi* and other alkenone-producing haptophytes in the Alboran Sea showed some variations over the annual cycle 1997–1998 with a minimum in winter and a maximum in May [*Bárcena et al.*, 2004]. Hence, the $U^{K'}_{37}$-derived SST likely represents annual mean SST with perhaps a somewhat larger influence of spring, although seasonal shifts over the last deglaciation cannot be discarded.

The strong correlation between LDI values and temperatures from the upper 30 m in the water column in globally distributed core-top sediments indicates that the photosynthetic nature of the biological source of the long-chain diols involved in the LDI [*Rampen et al.*, 2012]. Furthermore, for the global core-top data set, the best correlation of LDI with monthly satellite SSTs was obtained for the summer-autumn season [*Rampen et al.*, 2012]. Comparison of LDI-inferred and foraminiferal assemblage-derived SST records for the Southern Ocean suggested that the LDI reflects SST of the warmest months [*Lopes dos Santos et al.*, 2013]. Based on this limited data, the depth habitats of alkenone and diol producers in the western Mediterranean basin are probably similar (i.e., restricted to the surface waters), although differences in the timing of seasonal production may occur. A crossplot of $U^{K'}_{37}$- and LDI-derived SST estimates for the whole record shows that both proxies reflect, in general, similar SST estimates since the data points fall close to the 1:1 line (Figure 4) for both cores, although the somewhat lower $U^{K'}_{37}$-SSTs for the last 10 kyr in the 293G core clearly stand out. In general, the temperature range of the LDI-reconstructed SST over the last deglaciation (approximately 9–23°C) is slightly higher than that of $U^{K'}_{37}$ (approximately 11–22°C), and both ranges are comparable to that reconstructed for mean annual SST based on foraminiferal assemblages (approximately 9–19°C) [*Pérez-Folgado et al.*, 2003], although absolute values are slightly higher, suggesting that $U^{K'}_{37}$- and LDI-reconstructed SSTs are somewhat

Table 2. Average Estimated SST (°C) Obtained for Selected Time Periods Based on Organic Proxies in Cores 434G and 293G and Present-Day Annual Mean and Seasonal Temperatures (°C) of Seawater at 0 m Depth at Both Sites Obtained From the World Ocean Atlas on a 0.25° Grid [*Boyer et al.*, 2005]

		Time Interval				SST (°C)				
		Upper Sediment[a]	Average Last 1.0 cal kyr B.P.[b]	Average Last 5.0–1.0 cal kyr B.P.	Average Last 20.0–15.5 cal kyr B.P.	Annual Mean	Summer	Autumn	Winter	Spring
Core 434G	$U^{K'}_{37}$-SST (°C)	20.1	19.0 ± 0.5	21.2 ± 0.3[c]	-	18.0	21.3	18.0	15.4	17.4
	LDI-SST (°C)	17.3	-	20.9 ± 0.5[c]	-					
Core 293G	$U^{K'}_{37}$-SST (°C)	20.4	-	19.3 ± 0.3[d]	12.6 ± 0.5[d]	18.5	23.0	18.2	15.0	17.8
	LDI-SST (°C)	18.5	-	21.9 ± 0.5[d]	12.4 ± 0.5[d]					

[a]Equivalent to the last 30 cal years B.P. for core 434G and last 80 cal years B.P. for core 293G.
[b]Values from box core 436B ($n = 39$) [*Nieto-Moreno et al.*, 2013].
[c]Standard deviation ($n = 49$ for $U^{K'}_{37}$, $n = 13$ for LDI).
[d]Standard deviation ($n = 39$ for $U^{K'}_{37}$, $n = 10$ for LDI).

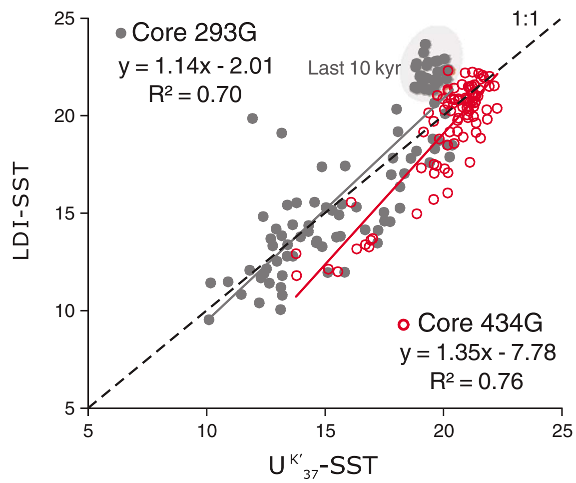

Figure 4. Cross correlation of LDI-SST with $U^{K'}_{37}$-SST for cores 293G (gray circles) and 434G (open red circles).

biased to the warmer season. Differences in the stronger seasonal range in SST between the Holocene (approximately 12°C) compared to the LGM (approximately 6°C) in the Alboran Sea, as reconstructed with foraminiferal assemblage transfer functions [*Pérez-Folgado et al.*, 2003], in combination with subtle shifts in the blooming season of alkenone and long-chain diol-producing algae may explain the differences in the $U^{K'}_{37}$- and LDI-SST records. Further studies on e.g., sediment traps quantifying annual fluxes of diols are needed to fully understand the possible effect of seasonality on the LDI.

A noteworthy characteristic of the Late Holocene LDI record is the decrease in reconstructed SST of approximately 4°C for the last 700 years in both cores (Figure 3c), a trend that is not seen for the $U^{K'}_{37}$ or foraminiferal isotope records. An identical trend was seen in the LDI in sediments recovered from a box core close to the position where core 434G was taken (data not shown). Possibly some of the long-chain diols were still present in a bound form in the most recent sediments since it is known that diols occur in eustigmatophytes in this form [*Volkman et al.*, 1992]. However, base and acid hydrolysis of the extracts of these surface sediments resulted in the release of long-chain diols with identical LDI values as for the free diols, ruling out the possible effect of diagenesis on LDI values. In good agreement with this, a similar drop in LDI values was not seen in the surface sediments from the Congo Basin [*Rampen et al.*, 2012]. Alternatively, the main season of production of the long-chain diols has shifted over the last 700 years resulting in lower reconstructed SSTs. Clearly, more research is required to fully understand this phenomenon.

4.2. Dual-Organic Proxy Temperature Reconstruction of the Alboran Sea: Paleoceanographic Implications

The good correspondence of our $\delta^{18}O$ record of the planktonic foraminifera *G. bulloides* in 293G core (Figure 3a) with the stable oxygen isotope stratigraphy from Greenland ice core records (North Greenland Ice Core Project) [*Lowe et al.*, 2008] supports our independent radiocarbon-based age model of this record. This allows to adopt the same timing and nomenclature for the climate events [see *Rodrigo-Gámiz et al.*, 2011]. Using this framework, we will discuss the observed SST changes using the two independent organic proxies.

4.2.1. From the Last Glacial Maximum to the Deglaciation

Reconstructed SSTs using the two different proxies are approximately 14°C during the LGM (20–18 cal kyr B.P.), with absolute temperature variations of ~0.5°C for $U^{K'}_{37}$, while LDI-reconstructed SSTs show a larger fluctuation of ~2.5°C (Figures 3b–3c). Lowest reconstructed SSTs at 9°C and 11°C are reached at 17.8 cal kyr B.P. This decrease in SST has been previously documented by records of $U^{K'}_{37}$ and the Mg/Ca ratio of benthic foraminifera in the Alboran basin with reconstructed SSTs as low as ~11°C [*Cacho et al.*, 2001, 2006; *Martrat et al.*, 2004], around 12°C with $U^{K'}_{37}$ and 9–10°C with MAT in the Levantine basin (see Figure 1 supporting information) [*Essallami et al.*, 2007; *Sicre et al.*, 2013]. This slight increase in $U^{K'}_{37}$-SST along the central Mediterranean is probably related to a reduced influence of the Atlantic water inflow.

At the beginning of the deglaciation, H1 depicts a clear minimum in the LDI-SST record (10°C) and the oxygen isotope record but not in the $U^{K'}_{37}$ record (Figure 3). This decrease in SST in the westernmost Mediterranean has been observed previously in $U^{K'}_{37}$ records [*Cacho et al*., 1999, 2002], in a shift in planktonic $\delta^{18}O$ values [*Sierro et al*., 2005; *Rodrigo-Gámiz et al*., 2011], by an increased relative abundance of the cold water foraminifera *N. pachyderma* (sinistral) [*Sierro et al*., 2005] and by maximum abundance of *E. huxleyi* shells (>4 μm) in the Alboran basin [*Pérez-Folgado et al*., 2003]. It is proposed to result from the inflow through the Strait of Gibraltar of colder and fresher North Atlantic water derived from the melting of icebergs [e.g., *Cacho et al*., 1999, 2002; *Sierro et al*., 2005; *Rodrigo-Gámiz et al*., 2011], combined with a meridional shift in the position of the polar front as suggested by other western and central Mediterranean records [e.g., *Kallel et al*., 1997a; *Siani et al*., 2001; *Essallami et al*., 2007; *Melki et al*., 2009].

At the end of the H1 event, a rapid warming trend is recorded in the LDI-SST record, reaching SSTs of 20°C at the Bölling period onset (14.7 cal kyr B.P.) (Figure 3c). A similar shift of almost 2‰ is observed in the $\delta^{18}O$ record (Figure 3a). This notable SST rise across this period has been recorded as a global warming interval preceding the Holocene using a suite of temperature proxies from a large set of SST records ([*Shakun et al*., 2012] and references cited therein) and is also apparent in SST data based on foraminiferal abundances in the Alboran basin [*Pérez-Folgado et al*., 2003]. Surprisingly, $U^{K'}_{37}$-SST remains constantly low (~12°C) during this period and only increases later (Figure 3b).

4.2.2. Climate Transitions in the Bölling-Alleröd and Younger Dryas

The $U^{K'}_{37}$-SST shows a rapid and abrupt SST increase from 12.5 to 18°C at the start of the Bölling and subsequently declines to SSTs of around 14°C at the end of the Alleröd (Figure 3b), while the LDI reveals a marked SST decline from 20 to 13.5 °C over this period (Figure 3c). The progressive decrease in LDI-SST from the Bölling onset to the beginning of the YD in the eastern Alboran, with a shift of about 7°C, is remarkably large compared to the smaller fluctuations recorded in $U^{K'}_{37}$ and, especially, $\delta^{18}O$ (Figures 3a–3c). A previous study based on Ba/Al ratio and the presence of biogenic barite from this record revealed the occurrence of high primary productivity during H1 and the YD, while lower productivity was recorded during the B-A period [*Rodrigo-Gámiz et al*., 2011]. Possibly, the changing nutrient concentrations during the B-A period and transition from and to cold conditions during the H1 and YD could have induced major changes in the blooming periods of the eustigmatophyte and haptophyte algae accounting for the discongruent changes in the LDI- and $U^{K'}_{37}$-derived SST records. The effect of environmental factors like nutrient availability on the LDI still needs to be constrained [*Rampen et al*., 2012].

The short-term temperature fluctuations during the B-A in the $U^{K'}_{37}$-SST for eastern record are comparable with those in the $\delta^{18}O$ profile of planktonic foraminifera (Figures 3a–3b). The availability of nutrients or oscillations in other environmental factors, causing seasonal changes in the coccolithophorid blooms in the east Alboran basin, may explain the rapid $U^{K'}_{37}$-SST fluctuations [cf. *Herbert*, 2003; *Bárcena et al*., 2004; *Prahl et al*., 2006]. More stable nutrient conditions in the upwelling zone in the western Alboran basin may have led to lower variability in the $U^{K'}_{37}$-SST in that area [e.g., *Sarhan et al*., 2000; *García-Gorriz and Carr*, 2001].

The late Alleröd period is documented by progressively declining SST trends in the $U^{K'}_{37}$- and LDI-SST records ending at the onset of the YD (approximately 12.9 cal kyr B.P.). The SSTs reconstructed for the start of the YD with the $U^{K'}_{37}$ and LDI vary in both Alboran records, i.e., 14°C and 12° for $U^{K'}_{37}$- and LDI-derived SSTs, respectively (Figures 3b–3c). This cooling event is much more pronounced than in the $\delta^{18}O$ record (Figure 3a). In any case, the coldest phase during the YD represents a relatively short period (300–600 years), in line with other $U^{K'}_{37}$ records from the western Mediterranean [*Cacho et al*., 2001]. The YD has been recognized in the western Mediterranean as a period that was not as cold as at higher latitudes [e.g., *Maslin et al*., 1995] and with an earlier warming than in Greenland [*Grootes et al*., 1993]. Several records from the Iberian sector and western Mediterranean region have documented the occurrence of climatic changes during the YD, pointing to an early cold/dry phase with a warmer/more humid episode during the latter phase [e.g., *Combourieu Nebout et al*., 2009; *Naughton et al*., 2007; *Rodrigo-Gámiz et al*., 2011]. However, in the eastern Mediterranean and northern Red Sea, organic proxies have shown a more gradual transition from the YD termination to the Holocene [*Arz et al*., 2003; *Castañeda et al*., 2010]. This coldest phase during the YD has been attributed to a southward propagation of the cold conditions throughout the Mediterranean basin [e.g., *Renssen et al*., 1996] with an intensification of the North Atlantic polar front by the strengthening of atmospheric cold conditions. The SST records reveal a warming from 14 to 20°C for $U^{K'}_{37}$ and 12 to 19°C for LDI with slightly lower temperatures for the eastern basin.

4.2.3. Holocene SST Fluctuations and Evolution From the West to the East Alboran Basin

In general, the $U^{K'}_{37}$-SST estimates in the western Alboran during the Holocene are similar to the alkenone record in the Gulf of Cadiz (19–22°C) [*Cacho et al*., 2001], while those in the eastern Alboran are in agreement with previous alkenone records and average temperatures inferred from MAT (~21°C) from nearby core sites [*Cacho et al*., 2001; *Jiménez-Espejo et al*., 2008]. The start of the Holocene (at 11,650 cal years B.P.) is recorded by a substantial SST increase of approximately 5°C until approximately 9.6 cal kyr B.P. as recorded by the LDI in both basins, mirroring the trend in the $\delta^{18}O$ profile (Figures 3a and 3c). In contrast, the $U^{K'}_{37}$ SST records only reveal a slight warming of 2°C that tends to be completed earlier (approximately 10.5 cal kyr B.P.). Another remarkable aspect is the progressive divergence in absolute SSTs derived from the $U^{K'}_{37}$ index in the western and eastern Alboran basin with values of about 19–22.5°C and 18–20.5°C, respectively (Figure 3b). SST fluctuations observed in the LDI records of both western and eastern basin are larger than those for $U^{K'}_{37}$, i.e., between 16–23.5°C and 16–22.5°C, respectively (Figure 3c), but here LDI-derived SSTs from the western basin are generally lower than those from the eastern basin, a trend that is opposite from that observed for $U^{K'}_{37}$-derived SSTs. The different responses of $U^{K'}_{37}$ between the two sites, as compared to LDI, suggest that there was more divergence in the haptophyte blooming season between both Alboran basins than for the growth season of the diol-producing algae. As mentioned before, the Alboran Sea presents a particular surface hydrological structure and circulation, with the development of the western and eastern Alboran gyres [*Millot*, 1999; *Vargas-Yáñez et al*., 2002]. The different hydrological conditions of both gyres have been previously described by particle fluxes and planktonic assemblages monitored with sediment traps during 1 year, denoting main productive events with nutrient variations and SST shifts due to the migration of both gyres during particular seasons [*Sanchez-Vidal et al*., 2004; *Hernández-Almeida et al*., 2011]. Specifically, the upwelling system located at the northern edge of WAG has undergone periodic southeastward advective displacements. In addition, major temperature anomalies, i.e., above or below the average monthly temperature, have been recorded in the Alboran basin [*López García and Camarasa Belmonte*, 2011]. Therefore, although the 434G core site is influenced by the superficial oceanographic circulation of the WAG and the upwelling area, this seasonal southeastward migration of colder waters to the eastern Alboran basin during late autumn and spring [*Sanchez-Vidal et al*., 2004] may explain the divergence in $U^{K'}_{37}$-SSTs revealed in both Alboran basins with rapid fluctuations and lower temperatures in the eastern record. This also agrees with the indication of an eastward migration of the WAG based on SST patterns [*Sánchez-Garrido et al*., 2013].

The most significant Holocene cooling documented in Greenland ice core records [e.g., *Alley et al*., 1997], as well as in western Mediterranean cores [*Cacho et al*., 2001; *Pérez-Folgado et al*., 2003] is the 8.2 kyr event. This cooling has been previously documented through the Mediterranean areas with a drop in $U^{K'}_{37}$-SST of 1–2°C in the Alboran Sea and a larger drop of 2.5–3°C in the Tyrrhenian Sea [*Cacho et al*., 2001]. This short-term cooling event was also evident in the western Mediterranean with a decrease in temperate water species (*Globigerinoides ruber white*) and a temperature drop of around 2°C using MAT on foraminiferal assemblages [*Pérez-Folgado et al*., 2003]. The 8.2 kyr event is recorded at the western site with a small decrease in $U^{K'}_{37}$ and in LDI, while less evident is in $U^{K'}_{37}$ and LDI records at the eastern site (Figures 3b–3c). Overall, the general differences between $U^{K'}_{37}$- and LDI- inferred SST values during the Holocene seem to be the result of differences in the production season of alkenone and long-chain diol producers, the divergence in the haptophyte blooming season between both basins, and the particular Alboran oceanographic circulation affecting SST.

5. Conclusions

The $U^{K'}_{37}$- and LDI-SST records have yielded a high-resolution SST reconstruction for the eastern and western Alboran Sea for the past 20 and 14 kyr, respectively. These results reinforce that the LDI is indeed a suitable temperature proxy in the western Mediterranean, providing complementary information on the paleoclimate and paleoceanographic evolution. The LGM and H1 depict minima in the $U^{K'}_{37}$- (12°C) and LDI-SST (10°C) records. A substantial SST increase (10°C) from H1 toward the Bölling onset is evident from the LDI-SST record, while the observed warming is more abrupt for the $U^{K'}_{37}$ and only starts in the Bölling, reaching values around 18°C. SSTs decrease during the B-A, and the first phase of the YD is recorded as a cold phase (~13°C-$U^{K'}_{37}$ and ~11°C-LDI). Early during the YD, SSTs start to rise with an overall SST increase of 5–6°C. During the Holocene, the organic proxies reflect different seasons with similar absolute SST values, ranging between 18 and 23°C, although a divergence in $U^{K'}_{37}$-SSTs between the two basins is observed. Higher absolute temperature values derived from $U^{K'}_{37}$ in the western (19–22°C) than in the eastern site (18–20°C) suggest seasonal southeastward advective displacements of the western Alboran gyre and related cold water from the upwelling area in the southern Iberian coast and divergence in the haptophyte blooming season between both basins.

Acknowledgments
This work was supported by Projects CGL2012-32659, CGL2009-07603, CTM2009-07715 (Secretaría de Estado de Investigación), 200800050084447 (MARM), Project RNM-5212, Research Group RNM-179 (Junta de Andalucía), and the Earth and Life Sciences Division of the Netherlands Organization for Scientific Research (NWO-ALW). We also thank the TTR program (UNESCO-Moscow State University) regarding the recovery of gravity cores 293G and 434G. We thank Anchelique Mets and Jort Ossebaar for laboratory assistance. We thank Hefter, an anonymous reviewer, and the Associate Editor Michel for their useful comments, which significantly improved the final manuscript.

References

Alley, R. B., P. A. Mayewski, T. Sowers, M. Stuiver, K. C. Taylor, and P. U. Clark (1997), Holocene climatic instability: A prominent, widespread event 8200 yr ago, *Geology*, *25*, 483–486, doi:10.1130/0091-7613(1997)025<0483:HCIAPW>2.3.CO;2.

Arz, H. W., J. Pätzold, P. J. Müller, and M. O. Moammar (2003), Influence of Northern Hemisphere climate and global sea level rise on the restricted Red Sea marine environment during termination I, *Paleoceanography*, *18*(2), 1053, doi:10.1029/2002PA000864.

Bárcena, M. A., J. A. Flores, F. J. Sierro, M. Pérez-Folgado, J. Fabres, A. Calafat, and M. Canals (2004), Planktonic response to main oceanographic changes in the Alboran Sea (Western Mediterranean) as documented in sediment traps and surface sediments, *Mar. Micropaleontol.*, *53*, 423–445, doi:10.1016/j.marmicro.2004.09.009.

Björck, S., et al. (1996), Synchronized terrestrial-atmospheric deglacial records around the North Atlantic, *Science*, *274*, 1155–1160.

Boussetta, S., N. Kallel, F. Bassinot, L. Labeyrie, J.-C. Duplessy, N. Caillon, F. Dewilde, and H. Rebaubier (2012), Mg/Ca-paleothermometry in the western Mediterranean Sea on planktonic foraminifer species *Globigerina bulloides*: Constraints and implications, *C. R. Geosci.*, *344*, 267–276, doi:10.1016/j.crte.2012.02.001.

Boyer, T., S. Levitus, H. Garcia, R. A. Locarnini, C. Stephens, and J. Antonov (2005), Objective analyses of annual, seasonal, and monthly temperature and salinity for the world ocean on a 0.25° grid, *Int. J. Clim.*, *25*, 931–945, doi:10.1002/joc.1173.

Brassell, S. C., G. Eglinton, I. T. Marlowe, U. Pflaumann, and M. Sarnthein (1986), Molecular stratigraphy: A new tool for climatic assessment, *Nature*, *320*, 129–133, doi:10.1038/320129a0.

Cacho, I., J. O. Grimalt, C. Pelejero, M. Canals, F. J. Sierro, J. A. Flores, and N. J. Shackleton (1999), Dansgaard-Oeschger and Heinrich event imprints in the Alboran Sea paleotemperatures, *Paleoceanography*, *14*, 698–705, doi:10.1029/1999PA900044.

Cacho, I., J. O. Grimalt, M. Canals, L. Sbaffi, N. J. Shackleton, J. Schönfeld, and R. Zahn (2001), Variability of the western Mediterranean Sea surface temperature during the last 25,000 years and its connection with the Northern Hemisphere climatic changes, *Paleoceanography*, *16*, 40–52, doi:10.1029/2000PA000502.

Cacho, I., J. O. Grimalt, and M. Canals (2002), Response of the Western Mediterranean Sea to rapid climate variability during the last 50,000 years: a molecular biomarker approach, *J. Mar. Syst.*, *33-34*, 253–272, doi:10.1016/S0924-7963(02)00061-1.

Cacho, I., N. J. Shackleton, H. Elderfield, F. J. Sierro, and J. O. Grimalt (2006), Glacial rapid variability in deep-water temperature and δ^{18}O from the Western Mediterranean Sea, *Quat. Sci. Rev.*, *25*, 3294–3311, doi:10.1016/j.quascirev.2006.10.004.

Castañeda, I. S., E. Schefuß, J. Pätzold, J. S. Sinninghe Damsté, S. Weldeab, and S. Schouten (2010), Millennial-scale sea surface temperature changes in the eastern Mediterranean (Nile River Delta region) over the last 27,000 years, *Paleoceanography*, *25*, PA1208, doi:10.1029/2009PA001740.

Comas, M. C., and M. K. Ivanov (2003), Alboran basin (Leg 3), in *Interdisciplinary Geoscience Research on the North East Atlantic Margin, Mediterranean Sea and Mid-Atlantic Ridge*, edited by H. Kenyon et al., pp. 51–71, IOC Technical Series UNESCO, Paris.

Comas, M. C., et al. (1996), Proceedings of the Ocean Drilling Program (ODP), Initial Reports 161, Mediterranean Sea II, Ocean Drilling Program, College Station, TX.

Combourieu Nebout, N., O. Peyron, and I. Dormoy (2009), Rapid climatic variability in the west Mediterranean during the last 25,000 years from high resolution pollen data, *Clim. Past*, *5*, 503–521, doi:10.5194/cp-5-503-2009.

Conte, M. H., A. Thompson, D. Lesley, and R. P. Harris (1998), Genetic and physiological influences on the alkenone/alkenoate versus growth temperature relationship in *Emiliania huxleyi* and *Gephyrocapsa oceanica*, *Geochim. Cosmochim. Acta*, *62*, 51–68, doi:10.1016/S0016-7037(97)00327-X.

Conte, M. H., M.-A. Sicre, C. Rühlemann, J. C. Weber, S. Schulte, D. Schulz-Bull, and T. Blanz (2006), Global temperature calibration of the alkenone unsaturation index (UK'37) in surface waters and comparison with surface sediments, *Geochem. Geophys. Geosyst.*, *7*, Q02005, doi:10.1029/2005GC001054.

de Leeuw, J. W., F. W. van de Meer, W. I. C. Rijpstra, and P. A. Schenck (1980), On the occurrence and structural identification of long chain unsaturated ketones and hydrocarbons in sediments, in *Advances in Organic Geochemistry 1979*, edited by A. G. Douglas and J. R. Maxwell, pp. 211–217, Pergamon Press, Oxford.

Elderfield, H., and G. Ganssen (2000), Past temperature and δ^{18}O of surface ocean waters inferred from foraminiferal Mg/Ca ratios, *Nature*, *405*, 442–445, doi:10.1038/35013033.

Emeis, K.-C., U. Struck, H.-M. Schulz, R. Rosenberg, S. Bernasconi, H. Erlenkeuser, T. Sakamoto, and F. Martínez-Ruiz (2000), Temperature and salinity variations of Mediterranean Sea surface waters over the last 16,000 years from records of planktonic stable oxygen isotopes and alkenone unsaturation ratios, *Palaeogeogr. Palaeoclimatol. Palaeoecol.*, *158*, 259–280, doi:10.1016/S0031-0182(00)00053-5.

Erez, J., and B. Luz (1983), Experimental paleotemperature equation for planktonic foraminifera, *Geochim. Cosmochim. Acta*, *47*, 1025–1031.

Essallami, L., M.-A. Sicre, N. Kallel, L. Labeyrie, and G. Siani (2007), Hydrological changes in the Mediterranean Sea over the last 30,000 years, *Geochem. Geophys. Geosyst.*, *8*, Q07002, doi:10.1029/2007GC001587.

García-Gorriz, E., and M. Carr (2001), Physical control of phytoplankton distributions in the Alboran Sea: A numerical and satellite approach, *J. Geophys. Res.*, *106*, 16,795–16,805, doi:10.1029/1999JC000029.

Gelin, F., I. Boogers, A. A. M. Noordeloos, J. S. Sinninghe Damsté, R. Riegman, and J. W. de Leeuw (1997), Resistant biomacromolecules in marine microalgae of the classes Eustigmatophyceae and Chlorophyceae: Geochemical implications, *Org. Geochem.*, *26*, 659–675, doi:10.1016/S0146-6380(97)00035-1.

González-Donoso, J. M., F. Serrano, and D. Linares (2000), Sea surface temperature during the Quaternary at ODP Sites 976 and 975 (western Mediterranean), *Palaeogeogr. Palaeoclimatol. Palaeoecol.*, *162*, 17–44, doi:10.1016/S0031-0182(00)00103-6.

Grauel, A.-L., A. Leider, M.-L. S. Goudeau, I. A. Müller, S. M. Bernasconi, K.-U. Hinrichs, G. J. de Lange, K. A. F. Zonneveld, and G. J. M. Versteegh (2013), What do SST proxies really tell us? A high-resolution multiproxy ($U^{K'}_{37}$, TEX^{H}_{86} and foraminifera δ^{18}O) study in the Gulf of Taranto, central Mediterranean Sea, *Quat. Sci. Rev.*, *73*, 115–131, doi:10.1016/j.quascirev.2013.05.007.

Grootes, P. M., M. Stuiver, J. W. C. White, S. Johnsen, and J. Jouzel (1993), Comparison of oxygen isotope records from the GISP2 and GRIP Greenland ice cores, *Nature*, *366*, 552–554, doi:10.1038/366552a0.

Herbert, T. D. (2003), Alkenones as paleotemperature indicators, *Treatise Geochem.*, *6*, 1–44, doi:10.1016/B0-08-043751-6/06115-6.

Herbert, T. D., L. C. Peterson, K. T. Lawrence, and Z. Liu (2010), Tropical ocean temperatures over the past 3.5 million years, *Science*, *328*, 1530–1534, doi:10.1126/science.1185435.

Hernández-Almeida, I., M. A. Bárcena, J. A. Flores, F. J. Sierro, A. Sanchez-Vidal, and A. Calafat (2011), Microplankton response to environmental conditions in the Alboran Sea (Western Mediterranean): One year sediment trap record, *Mar. Micropaleontol.*, *78*, 14–24, doi:10.1016/j.marmicro.2010.09.005.

Huguet, C., B. Martrat, J. O. Grimalt, J. S. Sinninghe Damsté, and S. Schouten (2011), Coherent millennial-scale patterns in $U^{K'}_{37}$ and TEX^{H}_{86} temperature records during the penultimate interglacial-to-glacial cycle in the western Mediterranean, *Paleoceanography*, *26*, PA2218, doi:10.1029/2010PA002048.

Jiménez-Espejo, F. J., et al. (2008), Detrital input, productivity fluctuations, and water mass circulation in the westernmost Mediterranean Sea since the Last Glacial Maximum, *Geochem. Geophys. Geosyst.*, *9*, Q11U02, doi:10.1029/2008GC002096.

Kallel, N., M. Paterne, L. Labeyrie, J. C. Duplessy, and M. Arnold (1997a), Temperature and salinity records of the Tyrrhenian Sea during the last 18,000 years, *Palaeogeogr. Palaeoclimatol. Palaeoecol.*, *135*, 97–108.

Kucera, M., et al. (2005), Reconstruction of sea-surface temperatures from assemblages of planktonic foraminifera: multi-technique approach based on geographically constrained calibration data sets and its application to glacial Atlantic and Pacific Oceans, *Quat. Sci. Rev.*, *24*, 951–998, doi:10.1016/j.quascirev.2004.07.014.

Lopes dos Santos, R. A., M. I. Spooner, T. T. Barrows, P. De Deckker, J. S. Sinninghe Damsté, and S. Schouten (2013), Comparison of organic ($U^{K'}_{37}$, TEX^{H}_{86}, LDI) and faunal proxies (foraminiferal assemblages) for reconstruction of late Quaternary sea-surface temperature variability from offshore southeastern Australia, *Paleoceanography*, *28*, 377–387, doi:10.1002/palo.20035.

López García, M. J., and A. M. Camarasa Belmonte (2011), Recent trends of SST in the Western Mediterranean basins from AVHRR Pathfinder data (1985–2007), *Global Planet. Change*, *78*, 127–136, doi:10.1016/j.gloplacha.2011.06.001.

Lowe, J. J., S. O. Rasmussen, S. Bjoerck, W. Z. Hoek, J. P. Steffensen, M. J. C. Walker, Z. C. Yu, and INTIMATE group (2008), Synchronisation of palaeoenvironmental events in the North Atlantic region during the Last Termination: A revised protocol recommended by the INTIMATE group, *Quat. Sci. Rev.*, *27*, 6–17, doi:10.1016/j.quascirev.2007.09.016.

Marlowe, I. T., J. C. Green, A. C. Neal, S. C. Brassell, G. Eglinton, and P. A. Course (1984), Long chain alkenones in the Prymnesiophyceae. Distribution of alkenones and other lipids and their taxonomic significance, *Br. Psychol. J.*, *19*, 203–216.

Martrat, B., J. O. Grimalt, C. Lopez-Martinez, I. Cacho, F. J. Sierro, J. A. Flores, R. Zahn, M. Canals, J. H. Curtis, and D. A. Hodell (2004), Abrupt temperature changes in the western Mediterranean over the past 250,000 years, *Science*, *306*, 1762–1765, doi:10.1126/science.1101706.

Martrat, B., J. O. Grimalt, N. J. Shackleton, L. de Abreu, M. A. Hutterli, and T. F. Stocker (2007), Four climate cycles of recurring deep and surface water destabilizations on the Iberian Margin, *Science*, *317*, 502–507, doi:10.1126/science.1139994.

Maslin, M. A., N. J. Schackleton, and U. Pflaumann (1995), Surface water temperature, salinity, and density changes in the northeast Atlantic during the last 45,000 years: Heinrich events, deep water formation, and climatic rebounds, *Paleoceanography*, *10*, 527–544, doi:10.1029/94PA03040.

Méjanelle, L., A. Sanchez-Gargallo, I. Bentaleb, and J. O. Grimalt (2003), Long chain n-alkyl diols, hydroxy ketones and sterols in a marine eustigmatophyte, Nannochloropsis gaditana, and in Brachionus plicatilis feeding on the algae, *Org. Geochem.*, *34*, 527–538, doi:10.1016/S0146-6380(02)00246-2.

Melki, T., N. Kallel, F. J. Jorissen, F. Guichard, B. Dennielou, S. Berné, L. Labeyrie, and M. Fontugne (2009), Abrupt climate change, sea surface salinity and paleoproductivity in the western Mediterranean Sea (Gulf of Lion) during the last 28 kyr, *Palaeogeogr. Palaeoclimatol. Palaeoecol.*, *279*, 96–113, doi:10.1016/j.palaeo.2009.05.005.

Millot, C. (1999), Circulation in the Western Mediterranean Sea, *J. Mar. Syst.*, *20*, 423–442.

Müller, P. J., G. Kirst, G. Ruhland, I. von Storch, and A. Rossell-Melé (1998), Calibration of alkenone paleotemperature index $U^{K'}_{37}$ based on core tops from the eastern South Atlantic and the global ocean (60ºN–60ºS), *Geochim. Cosmochim. Acta*, *62*, 1757–1771, doi:10.1016/S0016-7037(98)00097-0.

Naughton, F., M. F. Sánchez Goni, S. Desprat, J. L. Turon, J. Duprat, B. Malaize, C. Joli, E. Cortijo, T. Drago, and M. C. Freitas (2007), Present-day and past (last 25,000 years) marine pollen signal off western Iberia, *Mar. Micropaleontol.*, *62*, 91–114, doi:10.1016/j.marmicro.2006.07.006.

Nieto-Moreno, V., F. Martínez-Ruiz, V. Willmott, J. García-Orellana, P. Masqué, and J. S. Sinninghe Damsté (2013), Climate conditions in the westernmost Mediterranean over the last two millennia: An integrated biomarker approach, *Org. Geochem.*, *55*, 1–10, doi:10.1016/j.orggeochem.2012.11.001.

Nürnberg, D., J. Blima, and C. Hemleben (1996), Assessing the reliability of magnesium in foraminiferal calcite as a proxy for water mass temperatures, *Geochim. Cosmochim. Acta*, *60*, 803–814, doi:10.1016/0016-7037(95)00446-7.

Pérez-Folgado, M., F. J. Sierro, J. A. Flores, I. Cacho, J. O. Grimalt, R. Zahn, and N. Shackleton (2003), Western Mediterranean planktonic foraminifera events and millennial climatic variability during the last 70 kyr, *Mar. Micropaleontol.*, *48*, 49–70, doi:10.1016/S0377-8398(02)00160-3.

Prahl, F. G., and S. G. Wakeham (1987), Calibration of unsaturation patterns in long-chain ketone compositions for paleotemperature assessment, *Nature*, *330*, 367–369, doi:10.1038/330367a0.

Prahl, F. G., L. A. Muehlhausen, and D. B. Zahnle (1988), Further evaluation of long-chain alkenones as indicators of paleoceanographic conditions, *Geochim. Cosmochim. Acta*, *52*, 2303–2310, doi:10.1016/0016-7037(88)90132-9.

Prahl, F. G., A. C. Mix, and M. A. Sparrow (2006), Alkenone paleothermometry: Biological lessons from marine sediment records off western South America, *Geochim. Cosmochim. Acta*, *70*, 101–117, doi:10.1016/j.gca.2005.08.023.

Rampen, S. W., S. Schouten, S. G. Wakeham, and J. S. Sinninghe Damsté (2007), Seasonal and spatial variation in the sources and fluxes of long chain diols and mid-chain hydroxy methyl alkanoates in the Arabian Sea, *Org. Geochem.*, *38*, 165–179, doi:10.1016/j.orggeochem.2006.10.008.

Rampen, S. W., S. Schouten, and J. S. Sinninghe Damsté (2011), Occurrence of long chain 1,14 diols in *Apedinella radians*, *Org. Geochem.*, *42*, 572–574, doi:10.1016/j.orggeochem.2011.03.009.

Rampen, S. W., V. Willmott, J.-H. Kim, E. Uliana, G. Mollenhauer, E. Schefuß, J. S. Sinninghe Damsté, and S. Schouten (2012), Long chain 1,13- and 1,15-diols as a potential proxy for palaeotemperature reconstruction, *Geochim. Cosmochim. Acta*, *84*, 204–216, doi:10.1016/j.gca.2012.01.024.

Reimer, P. J., et al. (2009), INTCAL09 and MARINE09 Radiocarbon age calibration curve, 0-50000 years cal BP, *Radiocarbon*, *51*, 1111–1150.

Renssen, H., M. Lautenschlager, and C. J. E. Schuurmans (1996), The atmospheric winter circulation during the Younger Dryas stadial in the Atlantic/European sector, *Clim. Dyn.*, *12*, 813–824, doi:10.1007/s003820050145.

Rodrigo-Gámiz, M., F. Martínez-Ruiz, F. J. Jiménez-Espejo, D. Gallego-Torres, V. Nieto-Moreno, O. Romero, and D. Ariztegui (2011), Impact of climate variability in the western Mediterranean during the last 20,000 years: Oceanic and atmospheric responses, *Quat. Sci. Rev.*, *30*, 2018–2034, doi:10.1016/j.quascirev.2011.05.011.

Sánchez-Garrido, J. C., J. García Lafuente, E. Álvarez Fanjul, M. García Sotillo, and F. J. de los Santos (2013), What does cause the collapse of the Western Alboran Gyre? Results of an operational ocean model, *Prog. Oceanogr.*, *116*, 142–153, doi:10.1016/j.pocean.2013.07.002.

Sanchez-Vidal, A., A. Calafat, M. Canals, and J. Fabres (2004), Particle fluxes in the Almeria-Oran front: Control by coastal upwelling and sea surface circulation, *J. Mar. Syst.*, *52*, 89–106, doi:10.1016/j.jmarsys.2004.01.010.

Sarhan, T., J. García Lafuente, M. Vargas, J. M. Vargas, and F. Plaza (2000), Upwelling mechanisms in the northwestern Alboran Sea, *J. Mar. Syst.*, *23*, 317–331, doi:10.1016/S0924-7963(99)00068-8.

Sbaffi, L., F. C. Wezel, N. Kallel, M. Paterne, I. Cacho, P. Ziveri, and N. Shackleton (2001), Response of the pelagic environment to paleoclimatic changes in the central Mediterranean Sea during the Late Quaternary, *Mar. Geol.*, *178*, 39–62.

Schefuß, E., S. Schouten, and R. R. Schneider (2005), Climatic controls on central African hydrology during the past 20,000 years, *Nature*, *437*, 1003–1006, doi:10.1038/nature03945.

Schouten, S., E. C. Hopmans, E. Schefuß, and J. S. Sinninghe Damsté (2002), Distributional variations in marine crenarchaeotal membrane lipids: A new tool for reconstructing ancient sea water temperatures?, *Earth Planet. Sci. Lett.*, *204*, 265–274, doi:10.1016/S0012-821X(02)00979-2.

Send, U., J. Font, G. Krahmann, C. Millot, M. Rhein, and J. Tintoré (1999), Recent advances in observing the physical oceanography of the Western Mediterranean Sea: A review, *Prog. Oceanogr.*, *44*, 37–64, doi:10.1016/S0079-6611(99)00020-8.

Shackleton, N. (1967), Oxygen isotope analyses and Pleistocene temperatures re-assessed, *Nature*, *215*, 15–17, doi:10.1038/215015a0.

Shakun, J. D., P. U. Clark, F. He, S. A. Marcott, A. C. Mix, Z. Liu, B. Otto-Bliesner, A. Schmittner, and E. Brad (2012), Global warming preceded by increasing carbon dioxide concentrations during the last deglaciation, *Nature*, *484*, 49–54, doi:10.1038/nature10915.

Siani, G., M. Paterne, E. Michel, R. Sulpizio, A. Sbrana, M. Arnold, and G. Haddad (2001), Mediterranean Sea surface radiocarbon reservoir age changes since the Last Glacial Maximum, *Science*, *294*, 1917–1920, doi:10.1126/science.1063649.

Sicre, M.-A, G. Siani, D. Genty, N. Kallel, and L. Essallami (2013), Seemingly divergent sea surface temperature proxy records in the central Mediterranean during the last deglaciation, *Clim. Past*, *9*, 1375–1383, doi:10.5194/cp-9-1375-2013.

Sierro, F. J., et al. (2005), Impact of iceberg melting on Mediterranean thermohaline circulation during Heinrich events, *Paleoceanography*, *20*, PA2019, doi:10.1029/2004PA001051.

Sinninghe Damsté, J. S., S. W. Rampen, W. I. C. Rijpstra, B. Abbas, G. Muyzer, and S. Schouten (2003), A diatomaceous origin for long-chain diols and mid-chain hydroxy methyl alkanoates widely occurring in Quaternary marine sediments: Indicators for high nutrient conditions, *Geochim. Cosmochim. Acta*, *67*, 1339–1348, doi:10.1016/S0016-7037(02)01225-5.

Stuiver, M., and P. J. Reimer (1993), Extended ^{14}C data base and revised CALIB 3.0 ^{14}C Age calibration program, *Radiocarbon*, *35*, 215–230.

Stuiver, M., and P. M. Grootes (2000), GISP2 oxygen isotope ratios, *Quat. Res.*, *53*, 277–284, doi:10.1006/qres.2000.2127.

Ternois, Y., M.-A. Sicre, A. Boireau, M. H. Conte, and G. Eglinton (1997), Evaluation of long-chain alkenones as paleo-temperature indicators in the Mediterranean Sea, *Deep Sea Res., Part I*, *44*(2), 271–286, doi:10.1016/S0967-0637(97)89915-3.

Vargas-Yáñez, M., F. Plaza, J. García-Lafuente, T. Sarhan, J. M. Vargas, and P. Vélez-Belchí (2002), About the seasonal variability of the Alboran Sea circulation, *J. Mar. Syst.*, *35*, 229–248.

Versteegh, G. J. M., H. J. Bosch, and J. W. de Leeuw (1997), Potential palaeoenvironmental information of C_{24} to C_{36} mid-chain diols, keto-ols and mid-chain hydroxy fatty acids; A critical review, *Org. Geochem.*, *27*, 1–13, doi:10.1016/S0146-6380(97)00063-6.

Versteegh, G. J. M., J. H. F. Jansen, J. W. de Leeuw, and R. R. Schneider (2000), Mid-chain diols and keto-ols in SE Atlantic sediments: A new tool for tracing past sea surface water masses?, *Geochim. Cosmochim. Acta*, *64*, 1879–1892, doi:10.1016/S0016-7037(99)00398-1.

Volkman, J. K., G. Eghnton, E. D. S. Corner, and J. R. Sargent (1980), Novel unsaturated straight-chain C_{37}-C_{39} methyl and ethyl ketones in marine sediments and a coccolithophorid *Emiliania huxleyi*, in *Advances in Organic Geochemistry 1979*, edited by A. G. Douglas and J. R. Maxwell, pp. 219–227, Pergamon Press, Oxford.

Volkman, J. K., S. M. Barrett, G. A. Dunstan, and S. W. Jeffrey (1992), C_{30}-C_{32} alkyl diols and unsaturated alcohols in microalgae of the class Eustigmatophyceae, *Org. Geochem.*, *18*, 131–138, doi:10.1016/0146-6380(92)90150-V.

Volkman, J. K., S. M. Barrett, and S. I. Blackburn (1999), Eustigmatophyte microalgae are potential sources of C_{29} sterols, C_{22} - C_{28} n-alcohols and C_{28} - C_{32} n-alkyl diols in freshwater environments, *Org. Geochem.*, *30*, 307–318, doi:10.1016/S0146-6380(99)00009-1.